International Journal of Thermophysics, Vol. 13, No. 1, 1992

Pulse Techniques for Experimental Studies on Carbon at Extreme Temperatures[1]

M. A. Sheindlin[2]

Descriptions of the experimental methods and apparatus for investigations of the thermodynamic and optical properties of carbon are presented. It is stressed that the experimental difficulties in investigations at extremely high temperatures can be overcome in a combined study of different or similar properties using volume (slow electric explosion) and surface (laser) heating techniques. Special attention is given to the problem of high-speed pyrometry with millisecond to nanosecond time resolution. Some experimental results on properties of carbon up to 7000 K are presented.

KEY WORDS: graphite; high-speed measurements; high temperatures; laser heating; melting; pulse heating; pyrometry.

1. INTRODUCTION

The results of experimental investigations of carbon at high temperatures appear very contradictory [1–3]. One of the main reasons is the difficulties associated with the behavior of carbon in the region which covers three phases: solid (graphite), liquid carbon, and vapor. In order to perform detailed investigations of the behavior of carbon in the above-mentioned region, a number of different methods and apparatuses are required to permit the measurements in the temperature range unattainable by conventional methods. To perform investigations of refractory substances at extremely high temperatures, one should use methods involving laser heating, high-density resistive heating, etc.

[1] Paper presented at the Second Workshop on Subsecond Thermophysics, September 20–21, 1990, Torino, Italy.

[2] Institute for High Temperatures-IVTAN, USSR Academy of Sciences, Izhorzkaya 13/19, Moscow 127412, USSR.

0195-928X/92/0100-0095$06.50/0

The present paper describes the methods and apparatus developed at the Institute for High Temperatures of the USSR Academy of Sciences to study carbon in the high-temperature region. In developing the apparatus, the necessity of combining different techniques has been taken into consideration to overcome the difficulties which normally arise in the investigations in a new region where data and reference points lack.

2. METHOD AND APPARATUS FOR STUDY OF CARBON VAPOR PRESSURE UP TO 100 MPa

With regard to sublimation and vaporization of carbon, one should stress, first, the very high-temperature level, for instance, close to 4000 K at 0.1 MPa; second, the high value of vaporization enthalpy; and finally, the complex composition of saturated carbon vapor. Carbon differs from many substances by its sublimation up to 10-MPa pressure. As distinct from metals, for the investigation of graphite sublimation or vaporization, one must apply a technique which provides for the equilibrium of two phases up to very high pressures.

The proposed method is based on the evaporation caused by CW-laser heating with power densities in the range of 10^4–10^5 W · cm^{-2} with a buffer gas under high-pressure conditions. In this case, the rate of evaporation will be orders of magnitude lower than in the case of evaporation into vacuum.

The practical realization of this method consists of the following. The graphite sample was placed in a high-pressure cell (HPC) filled with buffer gas at a pressure p_a. At some moment of time, the laser heating was switched on. At the same time, the measurement of the specimen temperature as a function of time, $T(\tau)$, was started by using a fast pyrometer. After a few hundreds of milliseconds, the temperature reached the steady-state value or the "plateau" in the thermogram. The temperature which corresponds to the plateau was assumed to be equal to the temperature of vaporization or sublimation at the pressure p_a.

In doing the experiment, one had to solve a number of procedural problems, in particular, to define the lowest rate of evaporation one could maintain under the conditions of the experiment to satisfy the equation $p_V(T) = p_S(T)$, where p_S is the saturated vapor pressure and p_V the vapor pressure at the sample surface. The degree of nonequilibrium could be estimated using the Knudsen–Langmuir equation:

$$\dot{m} = \alpha_e(p_S - p_V)\sqrt{\mu_e/2\pi RT} \tag{1}$$

were $\dot{m}$ is the mass flow, α_e the effective vaporization coefficient, and μ_e the effective molecular weight. The value of $\dot{m}$ was estimated from the value of

the crater depth in the sample after the experiment. It is evident that the nonequilibrium can be neglected if $p_S - p_V \ll p_a$.

On the other hand, according to the proposed method, it should be assumed that $p_V = p_a$. It means that the partial pressure of the buffer gas at the sample surface should be close to zero. It is evident that the partial pressure profiles in the direction normal to the surface are governed by two competing processes, namely, hydrodynamic movement of vapor from the surface and diffusion flow of the buffer gas to the surface. The correlation between the two flows can be estimated using the dimensionless parameter

$$\beta = w_0/(D/r) \tag{2}$$

where w_0 is the vapor velocity on the surface, D the coefficient of relative diffusion of gas and vapor, and r the crater depth. If $\beta \gg 1$, then the rate of vapor flow is greater by far than the diffusion rate.

It follows from the above discussion that in performing the experiment, one must choose the optimal power density to provide for the vaporization rate in order to satisfy simultaneously two conditions: $\beta \gg 1$ and $p_V \approx p_S$.

The experimental setup is shown in Fig. 1. The main parts of the experimental system are: the HPC, Nd:YAG CW laser (500 W, $\lambda = 1.06\ \mu$m), high-speed wide-range micropyrometer, and multichannel spectrometer. All the instruments were connected to a computer-based data acquisition system.

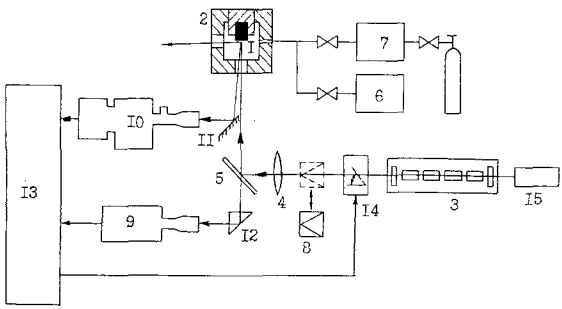

Fig. 1. Schematic of the isobaric laser heating apparatus. 1—Sample; 2—HPC, (high-pressure cell); 3—500-W YAG laser; 4—focusing lens; 5—semitransparent mirror; 6—vacuum pump; 7—membrane compressor; 8—absorbing cone power meter; 9—pyrometer; 10—multichannel spectrometer; 11—mirror; 12—prism; 13—data acquisition system; 14—shutter; 15—He–Ne laser.

Figure 2 shows the design of the HPC, which has the provision to permit laser heating and optical diagnostics through the hot high-pressure buffer gas.

The problem of great importance is that of temperature measurements because the heating thermogram contains information on the equilibrium temperature of the gas and the condensed phases. A pyrometer specially developed for use in this experiment has the following parameters: sighting ratio, 1:1000; temperature range, 1700–7000 K; measuring error, 0.2 to 2.0%, which corresponds to the lower and upper limits of the temperature scale; wavelength tuning range, 0.5–1.0 μm; and settling time, about 100 μs. The pyrometer utilized a diffraction grating monochromator for extraction and space splitting of quasi-monochromatic radiation fluxes.

The typical thermogram of heating in helium at a pressure of 100 MPa is shown in Fig. 3. According to the above, the use of thermograms for evaluating the temperature of vaporization or sublimation after examination of the crater depth helped make sure that the requirements of the method were satisfied.

The experimental investigation of vapor pressure was performed using various buffer gases: helium, neon, argon, and, for pressures lower then 10 MPa, krypton. No systematic dependence of the measurement results on the type of gas or sample was found. The experimental data on sublimation in the pressure range of 2×10^4–10^7 Pa [4] were approximated, using the least-squares method, by the following equation:

$$\ln p = 32.75 - 0.84 \times 10^5/T \tag{3}$$

where p is in Pa and T in K.

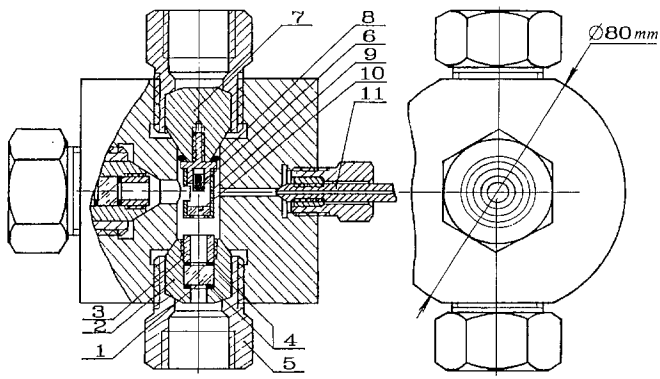

Fig. 2. The high-pressure cell (HPC). 1—Sapphire window; 2 and 7—plugs; 3 and 5—nuts; 4—Teflon gaskets; 6—sample; 8—rubber O-ring; 9—support; 10—protecting window; 11—gas inlet.

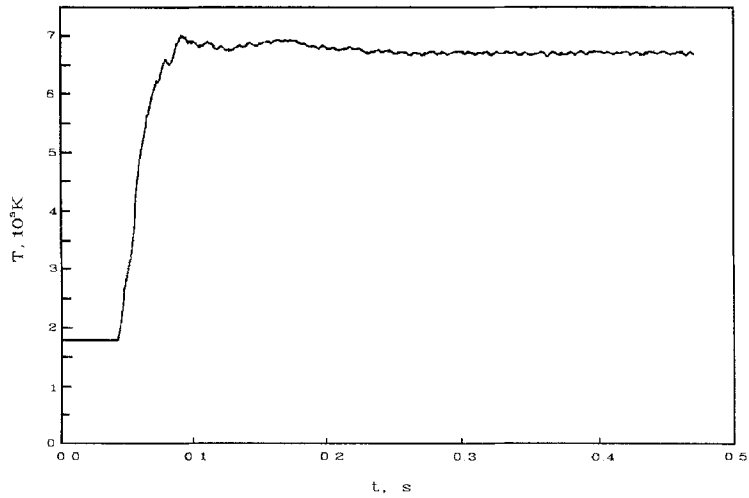

Fig. 3. Thermogram of graphite heating by laser in helium ($p_a = 100$ MPa).

For the evaporation of liquid carbon in the pressure range of 10–100 MPa, the following equation was obtained [5]:

$$\ln p = (11.14 \pm 0.80) - 10^4 \times (4.46 \pm 0.48)/T \tag{4}$$

where p is in MPa and T in K.

The total error in temperature of the thermogram "plateau" was estimated to be $\pm 5\%$.

3. THERMODYNAMIC PROPERTIES OF GRAPHITE IN THE VICINITY OF THE MELTING POINT

For the determination of the conditions of graphite melting, one needs to determine the melting temperature, T_m, and find the minimum pressure at which graphite can be melted (pressure at the triple point of carbon). The classic method for the determination of the phase transition due to melting is the examination of the temperature dependence of enthalpy. In order to obtain the $H(T)$ relationship, including the two-phase region, the "slow electrical explosion" method was employed. This method consists of Joule heating of the sample by high-density current over a time of the order of 1 ms.

Heating to the melting temperature T_m was performed in 2 to 0.5 ms under isobaric conditions at a gas pressure in the range 50 to 220 MPa. The measurement of enthalpy as a function of time was made by measuring

the voltage drop across some portion of the sample, $U(t)$, and of current through the sample as a function of time, $I(t)$:

$$H(t) = \frac{1}{m} \int_0^t [I(t)\, U(t) - \varepsilon_T \sigma S T(t)^4]\, dt \tag{5}$$

where ε_T is the hemispherical total emissivity, σ the Stefan–Boltzmann constant, S the surface area of the sample between potential contacts, and m the mass of sample between contacts. In measuring the surface temperature $T = T(t)$, the value of $H(T)$ is determined along with the current–voltage characteristics.

A schematic diagram of the experiment is shown in Fig. 4.

A pyrometer with microsecond resolution [6, 7], specially developed for use in this experiment, consists of a conventional optical system for the collection of the radiation from the desired region of the sample and a monochromatization part constructed in the same manner as that for the vapor pressure measurements. The pyrometer is characterized by its wide range of working temperatures, 2500–6000 K, made possible by the use of a silicon detector along with a precision logarithmic amplifier. When using a 12-bit ADC, the maximum error in the signal measurements amounted to about 0.06%.

The pyrometer was calibrated against a standard tungsten lamp at 0.65 μm (as a rule, only this wavelength was used) in the 1973–2473 K

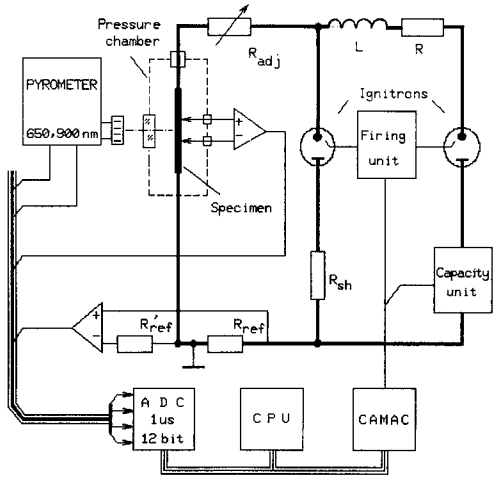

Fig. 4. Schematic of the apparatus for pulsed current heating of the sample.

range and against a blackbody in the 2000–3300 K range. The settling time of temperature readings to 99% was about 10 μs. The temperature resolution was 1.5 K at 2500 K and 5.5 K at 5000 K.

The sample prepared from highly oriented "quasi-single-crystal" UPV-ITMO pyrographite was a rod about 20 mm in length and about 1×1 mm in cross section with the basal plane along the sample. When sighting the pyrometer on the basal surface, the temperature measurement reproducibility was high. On the other hand, it was necessary to analyze the error introduced due to the unknown value of monochromatic emissivity of the a-surface ($\lambda = 0.65$ μm) and its temperature dependence.

Experiments on graphite melting were performed, as a rule, in the pressure range from 100 to 200 MPa and argon was used as the buffer gas. In shaping the heating current pulse, provision was made for the possibility of switching it off at a preset moment of time or on reaching a preset temperature.

Figure 5 shows a typical heating thermogram with brightness temperature recorded under conditions of continuous supply of energy to the sample. It is evident that, for a more detailed analysis, one needs to use experimental data on the emissivity of quasi-single-crystal graphite at least up to T_m. Therefore, one needs to perform a suitable investigation of emissivity and, on obtaining the necessary data, to generate the $H(T)$ relationship.

4. MEASUREMENTS OF MONOCHROMATIC EMISSIVITY OF PYROGRAPHITE AT BASE PLANE IN THE RANGE 2000–4000 K

To study the monochromatic emissivity of the a-surface of UPV-ITMO graphite, we have used a reflectometric method. In using the known

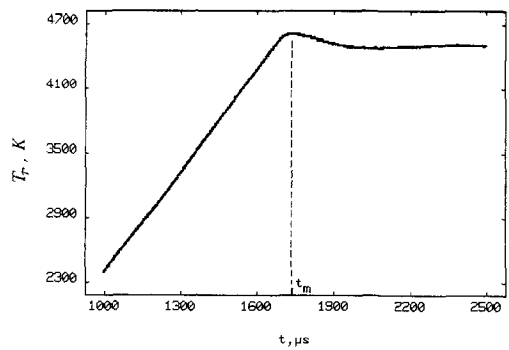

Fig. 5. Thermogram of pyrographite heating by high-density current to T_m (brightness temperature).

approach to the realization of the method of laser reflectometry based on continuous laser heating of the sample, difficulties are encountered in heating the graphite to temperatures close to T_m, which are due to intensive sublimation that occurs at temperatures above 3000 K.

In view of the above, we used a pulsed CO_2 laser for heating graphite with a power density of up to 2×10^7 W · cm^{-2}. Under heating with such a high-power density, graphite sublimes intensively but the temperature continues to rise because the power input exceeds the power consumed due to sublimation.

We used a CO_2 laser with a pulse of a characteristic shape made up of a leading spike with a half-height duration of about 250 ns and a "tail" slowly decreasing over a time of about 5 μs. The pulse energy was up to 3 J. Radiation was focused on the sample surface over a spot 2–4 mm in diameter. The degree of inhomogeneity of radiation over the heating spot was monitored and amounted to approximately 15%.

The experimental arrangement is shown schematically in Fig. 6 [8]. For recording the pulse shape, part of the radiation (about 1%) was directed to a special detector. In calibrating the pulse shape detector, the sample was replaced with a calorimeter measuring the total energy in the pulse.

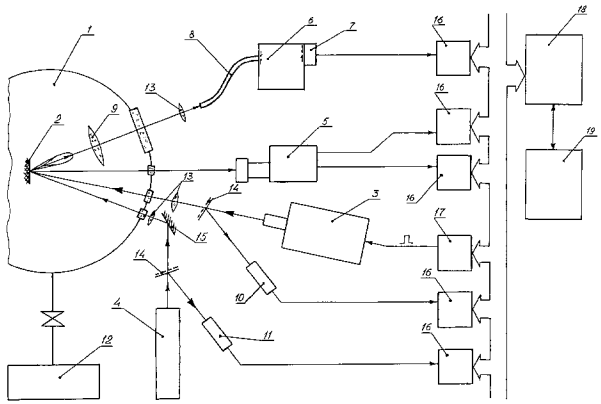

Fig. 6. Schematic of the apparatus for pulsed laser heating of the sample. 1—Vacuum chamber; 2—sample; 3—TEA–CO_2 laser; 4—He–Ne laser; 5—pyrometer; 6—monochromator; 7—Si detector; 8—optical fiber; 9—collecting lens; 10—CO_2 laser pulse detector; 11–He–Ne laser power meter; 12—vacuum pump; 13—lens; 14—light-splitting mirror; 15—mirror; 16—ADC (8 bit, 200 MHz); 17—pulse generator; 18 and 19—LSI-11/23 CPU with peripheral equipment.

In view of the short heating duration, the reflectivity should be measured with a time resolution of at least 100 ns. This causes additional difficulties in measuring the reflected signal on the wavelength of 0.63 μm (He–Ne laser was used as the source of radiation).

Since the reflectivity of UPV-ITMO graphite has a strongly pronounced specular component, reflected radiation was collected in a relatively small solid angle (about $\pi/24$) and focused by a lens to the input of a light guide. Its output end was used as the inlet aperture of a monochromator, ensuring spectral filtering of the radiation with a bandwidth of 0.5 nm. At the monochromator output, the radiation was measured and recorded with a fast photodiode and an amplifier transmitting the signal to the input of a fast ADC.

The sample was irradiated in a vacuum of 10^{-5}–10^{-6} Torr; this ruled out the possibility of atmospheric oxygen and nitrogen affecting the variation of the optical characteristics upon cooling of the sample, as well as precluding the formation of shocks occurring upon expansion of vapor into the buffer gas.

Temperature measurements were performed with the aid of a specially developed pyrometer [8]. It was designed using a high-speed photodiode and a fast linear current amplifier.

The reflection of He–Ne laser radiation from the *a*-surface of UPV-ITMO graphite was studied. Densities of the laser radiation were in the 1.0–2.2×10^7 W·cm^{-2} range. The upper value provided the laser breakdown threshold for the given experimental conditions.

The resulting reflectivity values were used to calculate, using Kirchhoff's law, the normal emissivity. The latter was in turn used to calculate the sample temperature from the measured brightness temperature.

Figure 7 shows the temperature dependence of reflectivity at 0.63 μm obtained by elimination of time from the $T(t)$ and $\rho_\lambda(t)$ relationships.

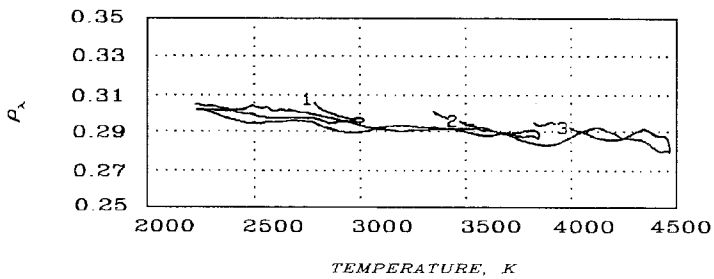

Fig. 7. Reflectivity as a function of temperature for three experiments on graphite corresponding to different laser energies.

The data for 25 experiments were treated using the least-squares method in the 2200–4500 K temperature range, yielding the following equation:

$$\rho_\lambda(T) = 0.32 - 8.30 \times 10^{-6} T \tag{6}$$

where T is in K.

5. PHASE DIAGRAM OF CARBON IN THE NEIGHBORHOOD OF THE TRIPLE POINT

The experimental results presented above enable one to solve the main problems of construction of the carbon phase diagram in the vicinity of the graphite–liquid–vapor triple point. As for sublimation and vaporization, the results are presented by Eqs. (3) and (4). The melting temperature was determined by linear extrapolation of the $H(T)$ relationship to the value of $H = H_m$ using Eq. (6) for the calculation of the true temperature. The value of $T_m = 5080 \pm 70$ K was obtaned by averaging the results of five successful experiments.

This value for the melting temperature is the highest of those obtained in experiments in direct investigation of melting [2] including the melting temperature $T_m = 4530 \pm 150$ K inferred from radiance temperature measurements by Cezairliyan and Miiller [9].

Based on the data reported in the literature, it is reasonable to accept the value 10 MPa for the triple-point pressure. In this case, from Eqs. (3) and (4) we have, respectively, $T_{tr}^{(sb)} = 4900 \pm 200$ K and $T_{tr}^{(vap)} = 5050 \pm 300$ K. Since the melting temperature depends weakly on pressure, one can consider $T_{tr}^{(ml)} = 5080 \pm 70$ K. So, from the author's point of view,

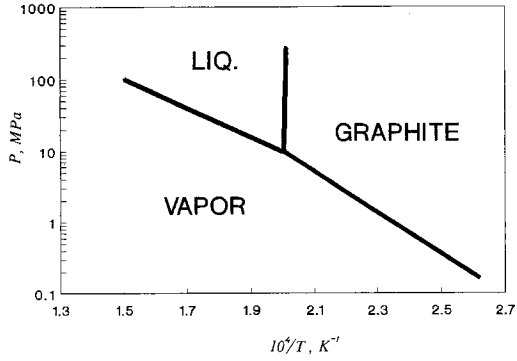

Fig. 8. Carbon phase diagram for the triple-point region.

for the triple-point temperature it is reasonable to accept the mean of these three values: $T_{tr} = 5015$ K.

The corresponding phase diagram of carbon in the triple-point region is shown in Fig. 8.

REFERENCES

1. F. P. Bundy, *J. Geophys. Res.* **85**:6930 (1980).
2. M. A. Scheindlin, *Teplofiz. Vys. Temp.* **19**:630 (1981) (in Russian).
3. F. P. Bundy, *Physica A* **156**:169 (1989).
4. V. N. Evseev, A. V. Kirillin, and M. A. Scheindlin, *Prom. Teploenerg.* **4**:87 (1982) (in Russian).
5. A. V. Kirillin, M. D. Kovalenko, M. A. Scheindlin, and V. S. Zhivopistsev, *Teplofiz. Vys. Temp.* **23**:699 (1985) (in Russian).
6. M. A. Scheindlin and V. N. Senchenko, in *Proceedings of Symposium on Major Problems of Present-Day Radiation Pyrometry* (Moscow, 1986), pp. 220–223.
7. M. A. Scheindlin and V. N. Senchenko, in *Thermal and Temperature Measurement in Science and Industry* (Institute of Measurement and Control, Sheffield, 1987), pp. 163–169.
8. S. V. Romanenko, M. A. Scheindlin, and A. A. Lebedev, IVTAN Preprint 1-269 (Moscow, 1989) (in Russian).
9. A. Cezairliyan and A. P. Miiller, *Int. J. Thermophys.* **11**:643 (1990).